World Journal of Advanced Research and Reviews
eISSN: 2581-9615 CODEN (USA): WJARAI
Cross Ref DOI: 10.30574/wjarr
Journal homepage: https://wjarr.com/

(RESEARCH ARTICLE)

Check for updates

Extraction of silica from rice husk for the production and optimization of metallurgical-grade silicon for potential engineering applications

Joshua A. Adam *, Innocent O. Oboh, Victor E. Etuk, Francis E. Okon and Peter E. Asangausung

Department of Chemical Engineering, Faculty of Engineering, University of Uyo, Uyo, PMB 1017 Uyo, Akwa Ibom State, Nigeria.

World Journal of Advanced Research and Reviews, 2025, 25(03), 2413-2433

Publication history: Received on 17 February 2025; revised on 27 March 2025; accepted on 29 March 2025

Article DOI: https://doi.org/10.30574/wjarr.2025.25.3.0961

Abstract

Conventional methods of silicon production; and carbothermic reduction, primarily rely on quartz or silica sand, which involves high-energy consumption and poses significant environmental challenges. Amidst this backdrop, the exploration of alternative sources for silicon extraction has become imperative. The utilization of rice husks which are considered renewable resources are produced every year in Nigeria. Despite its non-commercial value and causing environmental pollution, its ash content is rich in silica (SiO_2) and has become an economic potential source for the production of silicon. The high-purity metallurgical-grade silicon (MG-Si) was prepared by employing a successive acid leaching process followed by the reduction of rice husk ash (RHA) using magnesium as the reducing agent. The experiment was designed using a two-level-three-factor Box-Behnken Design (BBD), and 17 experimental runs were generated with operating process conditions of annealed temperature of 700-800^oC, ratio of HF:H_2SO_4 (1-9) and RHA: Mg ratio 1-1.5. The optimized MG-Si yield of 98.015 wt% was obtained at the process conditions of 799.365°C calcination temperature, 1:8.987 HF:H_2SO_4 ratio, and RHA: Mg ratio of 1:1.381. The produced MG-Si were characterized using XRF analysis and the results obtained indicated a MG-Si purity of 97.06wt% Si and 2.89wt% impurity respectively. Also, the XRF result showed that the impurities detected were Fe, K, Ca, Al, Ti, Cu, and Mg. The R^2 value of 0.9810 was achieved while the adjusted R^2 values of 0.9565 for the metallurgical grade silicon yield were in reasonable agreement with the predicted R^2 values of 0.9429, since their difference is less than 0.2. All of these validations showed that the experimental data for metallurgical grade silicon yield from rice husk ash matched the model's projected value accurately. Thus, optimizing the silicon production process has proven to be instrumental in achieving higher yields and better product quality. This not only enhances the overall efficiency of the production process but also contributes to the economic viability of silicon extraction from unconventional sources.

Keywords: Ash; Silica; Silicon; Leaching; Hydrometallurgy; Magnesiothermic; Rsm

1. Introduction

The pursuit of alternate and sustainable sources for silicon production has garnered significant attention in the dynamic field of engineering due to the environmental and economic consequences of conventional methods [1],[2],[3]. However, as the need for silicon in engineering applications grows, there is an increased interest in investigating alternate, sustainable sources of silicon from biomass [4], [5] and [6]. Silicon is an essential material in various engineering applications, including solar cells production, semiconductors, and alloys [7]. Silicon can be extracted from agricultural waste in the form of silica through several techniques (Figure 1). There are two types of silicon: solar-grade silicon and metallurgical-grade silicon [1] and [2].

* Corresponding author: Joshua A. Adam

Metallurgical-grade silicon (MG-Si) is a valuable metal with a wide range of industrial applications, including the production of hyper-pure "electronic grade" silicon (>99.99% Si), which is used in solar cells and the electronics industry, as well as a deoxidizer in the steel and aluminium industries, and an alloying element in the former [8],[2],[9] and [10]. The carbothermic reduction-smelting technique produces MG-silicon by reducing silica with carbon in a submerged arc furnace at temperatures ranging from 1300 to 2000°C under air pressure. The charge materials comprise a silicon source (quartz, sand, or quartzite) (Figure 1) and a standard reductant blend of coke, coal, charcoal, and wood chips [11], [12] and [13]. Equation (1) describes the reduction process.

$$SiO_2\ (s) + 2C_{(s)} \rightarrow Si(s) + 2CO_{(g)} \quad \text{.....Eq. (1)}$$

$$\Delta H_{2000^{\circ}C} = 687\ \text{kJ/mol.}$$

Alternately, metallothermic reduction employing metals including magnesium, calcium, barium, and aluminium as reductants can yield metallurgical-grade silicon as shown in Equation (2) [14], [15] and [1].

$$SiO_2 + 2Mg \rightarrow Si + 2MgO \quad \text{.....Eq. (2)}$$

Metallurgical-grade silicon MG-Si has various benefits in engineering applications [16] and [17]. Its high purity and outstanding mechanical properties make it an ideal material for usage in industries such as electronics, solar energy, and automobiles. Its versatility and sustainability makes it an essential tool for improving engineered material performance [18]. Silicon (Si) yield in the range of 99.9% has been attained by several researchers through magnesiothermic reduction of silica at a temperature between 600-950 ^{o}C [19] and [20]. However, conventional methods of silicon production; carbothermic reduction, primarily rely on quartz or silica sand, which involves high-energy consumption and poses significant Amidst this backdrop, the exploration of alternative sources for silicon extraction has become imperative. One such promising source is rice husk, an abundant byproduct stemming from rice milling processes [21].

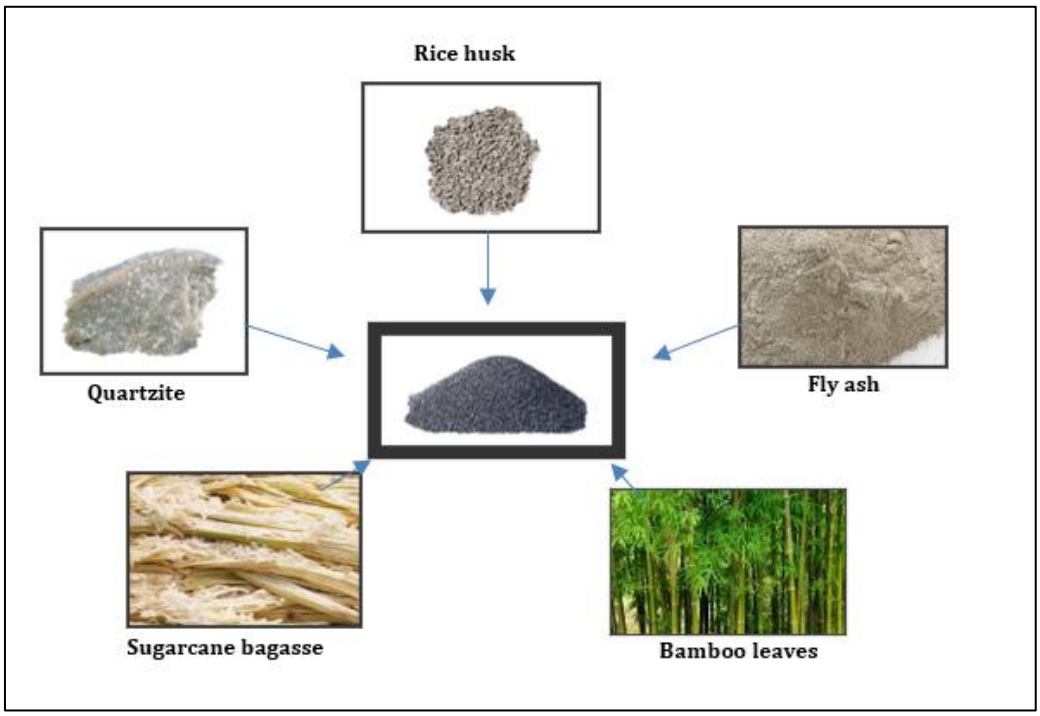

Figure 1 Sources of metallurgical grade silicon

Rice husk is known for its high silica content, it represents an attractive and renewable source for the production of metallurgical-grade silicon [22] and [23]. In the last few years, rice husk ash (RHA) has been used for a wide range of purposes. The most common use has been to create several types of amorphous silica, which are used in numerous industries [24] [25] and [26]. Scientists are particularly interested in the potential of amorphous silica, silicon tetrachloride zeolite, pure silicon, and silica nitride as raw materials for silica-based products [8]. Given that silica can be derived from (RHA), numerous studies have focused on its extraction from rice husks. This extraction process not

only yields valuable silica but also helps mitigate environmental pollution associated with the uncontrolled burning of rice husks [27] and [28]. Many researchers have developed techniques for extracting silica from rice husks. According to [29], silica can be extracted from rice husks through the processes of acid leaching. According to the Food and Agriculture Organization of the United Nations (FAO), Nigeria ranks as the leading rice producer in Africa, with an annual production of approximately 8,435,000 tons. It is followed by Egypt, Madagascar, Tanzania, and Mali [30]. On average, 20% of rice husk ash is produced from combusted rice husk, yielding 80-95% silica content [31]. Hence, this implies that Nigeria's rice production alone has the potential to generate approximately 170,000 tonnes of silica annually, which can be used for silicon production [22] and [32].

Numerous feasibility studies have explored the production of solar- and metallurgical-grade silicon from amorphous silica in rice husk ash through metallothermic reduction. Singh and Dhindaw [33] successfully obtained silicon with 6N purity by reducing white rice husk ash using magnesium at 800°C, followed by multiple acid-leaching steps. Later, Bose and Govindacharyulu [34] investigated the reduction of rice husk ash with magnesium at a lower temperature range of 600–650°C, but the resulting silicon had significantly lower purity compared to Singh and Dhindaw's findings [33]. Further research on magnesium reduction of rice husk ash for silicon production was conducted by Banerjee [35] and Ikram and Akhter [36]. Banerjee [35] used acid-leached rice husk ash mixed with magnesium powder and heated the mixture in a sealed graphite crucible within a muffle furnace. Following a similar methodology but using 4N purity magnesium, Ikram and Akhter [36] reduced rice husk ash at 620°C, achieving silicon with 99.95% purity after acid-leaching purification. Their findings underscored the potential of conventional refining methods to upgrade silicon to solar-grade quality, thereby bridging the gap between renewable resources and high-performance silicon applications [37]. Collectively, these studies illuminate the intricate process of harnessing rice husk ash as a sustainable feedstock for high-purity silicon production, highlighting both advancements and challenges in the quest for eco-friendly and economically viable silicon manufacturing processes [4] and [38]. Only a limited number of research groups have explored an alternative approach for synthesizing cost-effective solar-grade silicon from plant biomass like rice husk, which is rich in high-purity silica [11]; [34].

In recent years, statistical design tools like Design Expert have gained traction in optimizing complex processes by systematically exploring the multifaceted parameter space [39]. Design of Experiments (DOE) methodologies integrated with advanced statistical techniques enable researchers to identify significant factors, their interactions, and optimal conditions for maximizing desired outcomes [39]. Conventional approaches are time-consuming, highlighting the need for systematic optimization methodologies [40].

Furthermore, several research works showed that varying one variable at a time (OVAT) method was used to evaluate the impact of process variables. This method is time-consuming and requires an unreliable number of experiments [41]. In addition to these, the OVAT technique is not capable to optimize and achieve true optimal conditions in a multivariant system such as a metallurgical-grade silicon production process [42] and [43]. One of the experimental design techniques commonly used for process analysis and modeling is response surface methodology (RSM) [44].

Response Surface Methodology (RSM) is a highly effective statistical approach for optimizing processes in multivariable systems. It utilizes mathematical and statistical techniques for process modeling and analysis [45]. This method is particularly useful for optimizing systems where multiple parameters influence the response [46]. RSM enables the estimation of linear, interaction, and quadratic effects of process variables while also developing predictive models for process outcomes. The experimental data required depends on the chosen design, typically the central composite design (CCD) or the Box-Behnken design (BBD). These designs differ in the number of experimental runs needed and the combinations of factor levels tested. The Box-Behnken design is often considered more efficient and powerful than the central composite design (CCD) because it requires fewer experiments while effectively modeling most steady-state process responses [47]. Also, artificial neural networks (ANN) have been recognized as a reliable tool for modeling complex processes involving nonlinear data. While ANN offers a robust and dependable modeling approach, it requires an additional perturbation method for sensitivity analysis [48]. This necessity has driven research into combining ANN with other algorithms, an approach that has gained significant attention and has been successfully applied as a modeling and optimization tool for solving complex and nonlinear problems [49].

However, studies on metallurgical-grade silicon production using RSM and ANN to provide an explicit understanding of the effect of process variables on MG-Si yield have not been documented to the best of the author's knowledge. Thus, the present work aimed to investigate the potential of extracting silica from rice husks for MG-Si production and develop a predictive explicit model using RSM and ANN [50].

2. Materials and methods

Rice husk was obtained from a local rice mill Company in Cross River State, Nigeria. All the other chemicals were of analytical reagent grade and were acquired both within and outside Akwa Ibom State from various chemical stores in Nigeria. Figure 2 shows the flow diagram employed for the production of metallurgical-grade silicon from rice husk

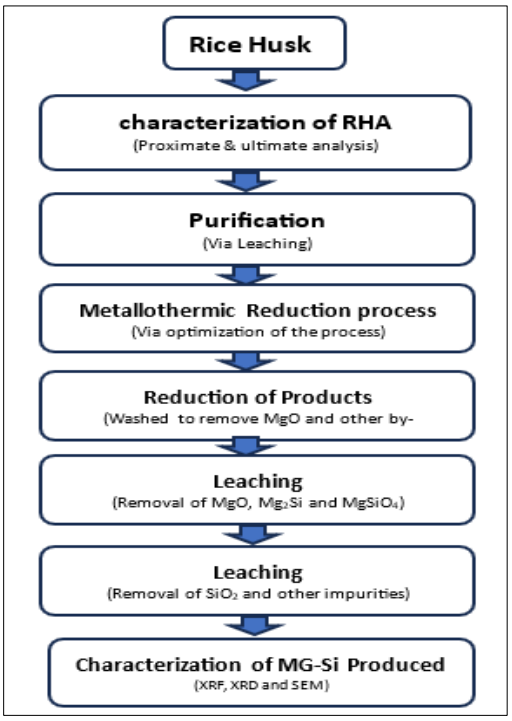

Figure 2 Flow diagram for MG-Si Production

2.1. Sample Preparation (Rice Husk)

The rice husk (RH) sample was washed thoroughly with de-ionized water to remove the soluble particles, dust, dirt, and other sand particles present in the husk. The samples after washing were drained of water, sun-dried (Figure 4), and oven-dried at 105 ^{o}C for 2 hours to constant weight. Figure 3 shows the schematic process for the preparation of silicon from raw rice husk.

Figure 3 A schematic process for the preparation of silicon from raw rice husk

Figure 4 Sundried Rice Husk

2.1.1. Purification of Rice Husk (Acid Leaching)

The method of Olawale. [2] was adopted in this step. 184.68g of the prepared rice husk was added to 1500 ml of 1N HCl for 2 hours in a beaker and heated up to a temperature of 100 ^{o}C for 2hrs with constant mixing, and it was then left for 3 hours to cool. The supernatant was then drained and washed repeatedly with plenty of de-ionized water to remove the acid retained to obtain a pH of 7.0, the rice husk was then filtered out and dried in an oven at 105 ^{o}C for 4 hours. Figure 5 shows the rice husk sample after leaching.

Figure 5 Leached Rice Husk

2.1.2. Extraction of Silica from Prepared Rice Husks

The method of Larbi, [5] was adopted in this step. The prepared rice husk was burned in a Muffle furnace into ash at 400 ^{o}C for 1 hour (Figure 6). It was further heated for 4 hours at a temperature of 700 ^{o}C to obtain (RHA) (see Figure 7); thereafter, it was cool inside the furnace before removing and then analyzed for silica yield using Equation 3.

$$Rice\ Husk\ Ash\ recovery\ (\%) = \frac{\text{Mass of Rice Husk Ash}}{\text{Mass of Rice Husk used}} \times 100 \quad \text{.....Eq. (3)}$$

Figure 6 Carbonized Rice husk

2.1.3. Purification of RHA (Hydrometallurgy process)

To remove impurities present in the rice husk ash (RHA), a low-cost process known as the hydrometallurgy leaching treatment process was adopted. This treatment involves the addition of 80 cm^3 of 16M HNO_3 to 60 g RHA and heating at 700°C for an hour. The product was rinsed in deionized water, filtered, and dried. The sample then underwent digestion using 5M HCl acid for 2 hrs at 95 °C with constant agitation. Whitman paper was used in filtering the residues of the digested sample and then rinsed again with deionized water until the rinse water had a pH of between 7 and 7.4. The solid was filtered and dried in an oven for 1 hr at 105°C [1]. The extraction yield was evaluated using Equation 4. Figure 7 shows the purified rice husk ash being weighed.

$$\text{Silica Yield (\%)} = \frac{Mass\ of\ Produced\ Silica}{Mass\ of\ Rice\ Hush\ Ash} \times 100 \qquad \text{..... Eq. (4)}$$

Figure 7 Purified Rice Husk Ash

2.2. Metallurgical-Grade Silicon (MG-Si) Production

The leached rice husk ash from the hydrometallurgy process was subjected to a metallothermic reduction process for metallurgical-grade silicon production. Table 5 shows the process conditions followed to produce the metallurgical-grade silicon. The produced metallurgical-grade silicon produced is shown in Figure 8.

Figure 8 Metallurgical-grade Silicon Produced

2.2.1. Metallothermic Reduction Process

The amorphous silica from leached rice husk ash (LRHA) was subjected to a metallothermic reduction process for metallurgical-grade silicon production. The purified silica was homogeneously pulverized using agate mortar and thoroughly mixed with magnesium powder (magnesium turning (99% purity) at a specified ratio of RHA:Mg, HF:H_2SO_4, and residence time and annealed in a furnace at the specified temperature by RSM in Table 4. The mixture was then cooled to room temperature before it was removed from the furnace.

2.2.2. Leaching of Reduction Products

Leaching was carried out twice. The first was to selectively leach out magnesium by-products and other impurities via 2M HCl volume of 15 ml at a temperature of 70 °C for a period of 1hr. The final leaching was HF and H_2SO_4 leaching, and it was carried out at different concentrations as specified by RSM in Table 5. The reduced sample was acid-leached with a mixture of concentrated HF and H_2SO_4 at a specified ratio to remove impurities like MgO and other impurities that were present in the form of silicate or oxide. Leaching time and temperature were kept at 1hr and 70^{o}C, respectively. The product was washed with de-ionized water, filtered, and the residues oven-dried at 100^{o}C for 1 hr to obtain pure MG-silicon [1]. The silicon obtained was then examined with XRF and SEM Spectra and was compared with the standard silicon.

$$SiO2 + 2Mg \rightarrow Si + 2MgO \quad \text{..... Eq. (5)}$$

The acid was introduced into the reduced product in a closed beaker. The leaching procedure is adopted from the work of [1] to remove Mg, MgO, and unreacted SiO_2. The process was represented by the chemical formula in Equation 5.

2.3. Experimental Design and Optimization of the MG-Silicon Production Process

The process was carried out following Design of Experiment specification. The statistical analysis was performed according to the Response Surface Methodology (RSM) using Design Expert version 13 (Stat-Ease Inc, Min-neapolis, MN, USA). Box Behnken Design (BBD) was used for the optimization of MG-silicon production to examine the combined effect of the three different factors (independent variables): Temperature (^{o}C), leaching agent concentration, and ratio of reducing agent RHA:Mg on the yield of metallurgical-grade silicon (Response). The data specification from Design of Experiment as shown in Table 5 was followed accurately to determine the combined effect of the independent variables and was fitted into a second-order model (Equation 6) to correlate the response variable to the independent variable. A total of 17 experimental runs were generated, as shown in Table 5. The general form of the second-degree polynomial Equation is as follows:

$$\gamma = \beta_0 + \sum_{j=1}^{k} B_j x_j + \sum_{i<j} \sum B_{ij} x_i x_j + \sum_{j=1}^{k} B_{ij} x_j^2 + \varepsilon \quad \text{.....Eq. (6)}$$

Where Y is the predicted response, β_o, B_j, B_{ij}, and constant coefficients; xi and xj are the coded independent variables or factors: Ɛ is random error. The effect of the process variables on the yield of metallurgical-grade silicon was calculated, and their respective significance was evaluated by ANOVA test. P-values were used as a yardstick for measuring the significant regression coefficients.

2.4. Characterization of Rice Husk Ash

The rice husk used for the experiment was subjected to moisture content, volatile matter, fixed carbon, and ash content analysis.

2.4.1. Moisture content

The raw rice husk was placed in a crucible, and its weight was measured both with and without the husk. The crucible containing the rice husk was then dried in an oven at 105°C for four hours. After drying, the sample was removed, allowed to cool, and re-weighed until a constant weight was achieved. Finally, the final weight was recorded and compared with the initial measurement. The percentage of moisture content of the rice husk was calculated using Equation (7).

$$\%Moisture\ Content = \frac{M_1 - M_2}{M_1} \times 100 \text{..... Eq. (7)}$$

Where: M_1=Weight of sample before drying (g); M_2=Weight of sample after drying (g)

2.4.2. Volatile matter

The crucible and its cover were weighed both with and without the rice husk sample. The muffle furnace was then preheated to 500°C. The sample was placed in a sealed crucible and heated in the muffle furnace at 500°C for five minutes. After heating, the crucible was cooled in a desiccator and re-weighed. The volatile matter content was determined by comparing the sample's weight before heating (V_1) and after heating (V_2). The percentage of volatile matter in the sample was calculated using Equation 8.

$$Volatile\ Matter\ \% = \frac{V_1 - V_2}{V_1} \times 100 \qquad \text{.....Eq. (8)}$$

Where: V_1= Weight of sample before heating (g); V_2=Weight of sample after heating (g)

2.4.3. Ash Content

The muffle furnace was preheated to 500°C. The crucible was weighed both with and without the rice husk sample. The sample was then placed in an open crucible and heated at 500°C for two hours in the furnace. After heating, the crucible was transferred to a desiccator and left to cool to room temperature before being re-weighed. The ash content of the sample was determined by comparing its weight before and after heating. The percentage of ash in the sample was calculated using Equation 9.

$$Ash\ Content\ \% = \frac{A_2}{A_1} \times 100 \text{.....} \quad \text{Eq. (9)}$$

Where: A_1=Weight of the sample before heating (g); A_2=Weight of the sample after heating (Ash) (g)

2.4.4. Fixed carbon content

The fixed carbon content was calculated by deducting the combined volatile matter and ash content from 100. The resulting value represented the percentage of fixed carbon present in the sample. The percentage of fixed carbon content in the sample will be calculated using Equation 10.

Fixed carbon (%) = 100 - (moisture% + ash% + volatile matter %) .....Eq. (10)

2.5. Characterization of the Produced MG-Si

The produced MG-silicon obtained was subjected to SEM and XRF analysis to determine its surface morphology and elemental composition, respectively.

2.6. Model performance Indices test

The predictive performance of the ANN and RSM models was evaluated using various performance indices to determine which model best aligned with the experimental data. Seven high-accuracy statistical error functions, listed in Table 1, were employed for this analysis. The selected evaluation criteria were based on the characteristics of the data set used [51]. Additionally, a comparative parity plot was generated to highlight specific deviation points between the predictions of the RSM and ANN models and the experimental data

Table 1 Statistical Error Functions

Error function	Equation
Hybrid fractional error function	$HYBRID\ (\%) = \frac{1}{N-P}\sum \frac{\left[P_{R,J,exp} - P_{R,J,cal}\right]^2}{P_{R,J,exp}} \times 100$
Average relative error	$ARE\ (\%) = \frac{100}{N}\sum_{i=1}^{N} \frac{P_{R,J,exp} - P_{R,J,cal}}{P_{R,J,exp}} \times 100$
Correlation coefficient	$R^2 = \frac{\left(\sum_{i=1}^{N} P_{R,J,cal} - P_{R,J,exp,ave}\right)^2}{\sum_{i=1}^{N}\left(P_{R,J,cal} - P_{R,J,exp}\right)^2 + \left(P_{R,J,cal} - P_{R,J,exp}\right)^2}$

Marquardt's percentage standard error deviation	$MPSED\ (\%) = \sqrt{\frac{\sum\left(\frac{\left[P_{R,J,exp} - P_{R,J,cal}\right]^2}{P_{R,J,exp}}\right)}{N-P}} \times 100$
Absolute average relative error	$AARE\ (\%) = \frac{1}{N}\sum_{i=1}^{N}\frac{P_{R,,\exp\,(i)} - P_{R,,cal(i)}}{P_{R,exp(i)}} \times 100$
Adjusted R^2	$Adj\ R^2 = 1 - \left((1-R^2) \times \frac{N-1}{N-P-2}\right)$
Root mean square error	$RMSE = \sqrt{\frac{1}{N}\sum_{i=1}^{N}\frac{\left[P_{R,\exp\,(i)} - P_{R,cal(i)}\right]^2}{P_{R,exp(i)}}}$

Source: [52]

3. Results and discussion

Table 2 Proximate Analysis for Rice Husk

Proximate	**Values (%)**
Moisture Content	9.2
Ash Content	22.9
Volatile Matter	65.4
Fixed Carbon Content	2.5

3.1. Scanning electron microscopy (SEM)

The SEM micrographs in Figure 9 demonstrate that the MG-Si obtained consists largely of spongy material with pores. The likely cause of the observed porosity is that acids leach out magnesium compounds and SiO_2 from the reduction product, thereby producing voids, a similar trend was also observed in the work of [15].

3.2. X-ray fluorescence (XRF)

The MG-silicon was chemically analyzed by XRF to determine its purity. The results are summarized in Table 3 and 4. The MG-Si product contained about 97.06% Si and 2.89 % impurity, with traces of other elements. It is clear that the MG-Si product had no traces of P, and it is noteworthy that no boron was detected. Most impurities detected were Mg, Fe, Al, and Ti, these may be attributed to the crucible and fabricated iron mold used during the ashing process. Iyen *et al.* [1] reported similar results.

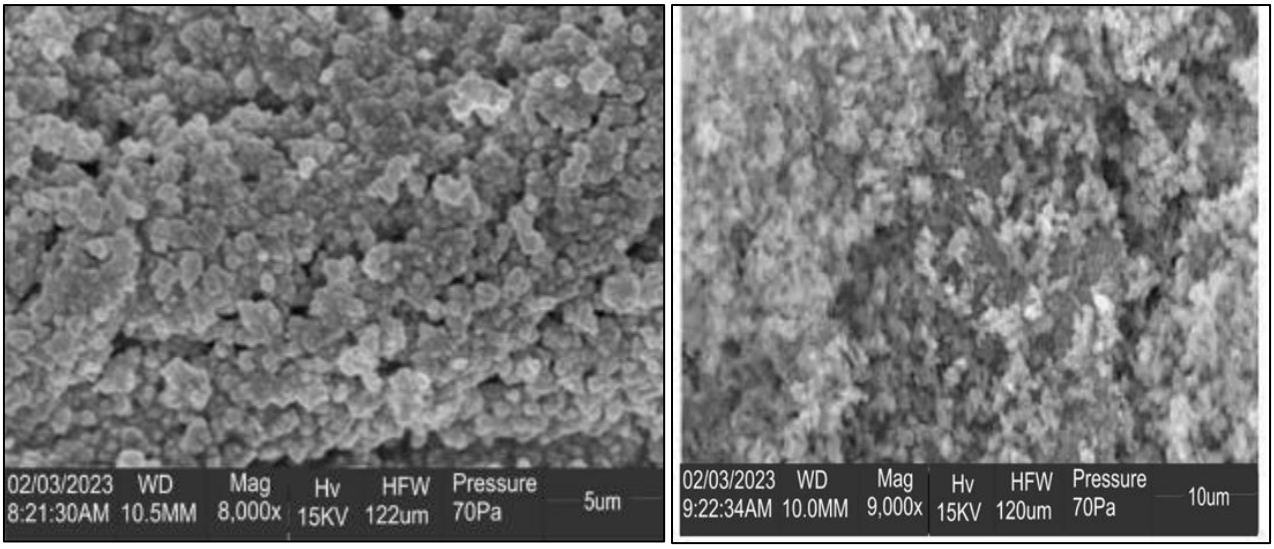

Figure 9 Scanning Electron Microscopy of (MG-Si) derived from rice husk ash (a) before leaching and (b) after leaching

Table 3 Chemical analysis of the RHA before and after leaching using XRF spectrometry

Compound	**SiO_2**	**K_2O**	**CaO**	**MnO**	**MgO**	**Al_2O_3**	**TiO_2**	**Fe_2O_3**	**P_2O_5**	**CuO**	**SO_3**	**ZnO**	**Ag_2O**	**Cl**	**Total impurity**
Before leaching wt (%)	90.636	0.266	1.925	0.064	1.653	1.362	0.129	0.667	0.318	0.51	0.799	0.021	0.003	2.089	9.364
After leaching wt %	94.224	0.152	0.805	0.031	0.000	1.546	0.123	0.161	0.028	0.043	0.715	0.010	0.002	2.142	5.776

Table 4 Quantitative Analysis of the Derived MG-Si Using X-ray fluorescence (XRF)

[1]	**Elements**	**[2]**	**Si**	**[3]**	**Al**	**[4]**	**K**	**[5]**	**Ca**	**[6]**	**Mg**	**[7]**	**Cu**	**[8]**	**Fe**	**[9]**	**Ti**	**[10]**	**Total Impurity**
[11]	MG-Si (wt %)	[12]	97.06	[13]	0.54	[14]	0.21	[15]	0.07	[16]	1.09	[17]	0.05	[18]	0.91	[19]	0.02	[20]	2.89

The XRF analysis results for MG-Si derived from rice husk ash after leached are presented in Table 3. Also, the results indicate a Silicon (Si) yield of 97.06wt% and 2.89wt % impurity respectively, which is slightly below the value reported in the literature, Larbi, [5] obtained 97.3wt%, similarly, Benedict and Karen, [32] reported 98.66wt%. Also, the obtained value in this study is a close range to the required purity level for metallurgical-grade silicon as reported by Pizzini, [7]. Looking at the impurities detected Fe, K, Ca, Al, Ti, Cu, and Mg were observed using XRF. The high amount of Al and Mg are due to Al introduction into the sample from the alumina crucible during heating and reaction of Si with an excess of Mg during the reduction process respectively.

3.3. Statistical Analysis of RSM Model Result

3.3.1. ANOVA

The results from the experimental data were analyzed using the regression analysis tool in Design Expert 13 and Table 5 shows the ANOVA results for the quadratic model of (MG-Si) Yield. The performance of a model in making predictions can be measured using its predicted R^2. To figure out how well the model worked, the mean square, sum of squares, degree of freedom (DOF), P value, and F value were each calculated. Table 6 shows the ANOVA result for the (MG-Si) Yield model. According to the results of the variance analysis, an F value that is more than 2.6 suggests a more accurate estimation of the parameters [42]. The results of the ANOVA for the Quadratic Model and the Significant Parameters of P-value are presented in Table 6. A P-value below 0.05 implies that there is a statistical significance between the terms in the model. Since the F value of the model is 40, it can be concluded that it is statistically significant. Also, the terms with P values below 0.05 are considered significant. In this case, A, B, B^2, and C^2 are significant model terms. The R^2 value for the response variable was 0.981, indicating that 98.1% of the total variance was well explained by the model. Since the adequate precision value of 23.6343 is more than 4, it may be concluded that this response was more accurate and trustworthy. Also, it was observed that factor A has the highest sum of square value (40.50), followed by B (28.13) and lastly C (1.13). This is in agreement with the findings of this indicate that calcination temperature and HF:H_2SO_4 ratio collectively has the highest influence on the (MG-Si) Yield.

Table 5 Experimental Factors and the Corresponding Metallurgical Silicon (MG-Si) Yield

		Factor 1	**Factor 2**	**Factor 3**	**Response 1**
Std	Run	A:Calcination Temperature	B:Ratio of HF:H_2SO_4	C:Ratio of RHA:Mg	MG-Si Yield
		(^oC)			%
17	1	750	5	1.5	94
15	2	750	5	1.5	93
14	3	750	5	1.5	94
6	4	800	5	1	95
4	5	800	9	1.5	98
8	6	800	5	2	95
9	7	750	1	1	91
13	8	750	5	1.5	93
3	9	700	9	1.5	94
11	10	750	1	2	92
16	11	750	5	1.5	94
2	12	800	1	1.5	95
12	13	750	9	2	96
1	14	700	1	1.5	90
7	15	700	5	2	91
5	16	700	5	1	90
10	17	750	9	1	95

Table 6 ANOVA for Quadratic Model and the Significant Parameters of P-Value

Source	**Sum of Squares**	**df**	**Mean Square**	**F-value**	**p-value**	

Model	74.79	9	8.31	40.11	< 0.0001	significant
A-Calcination Temperature	40.50	1	40.50	195.52	< 0.0001	
B-Ratio of HF:H_2SO_4	28.13	1	28.13	135.78	< 0.0001	
C-Ratio of RHA:Mg	1.13	1	1.13	5.43	0.0526	
AB	0.2500	1	0.2500	1.21	0.3083	
AC	0.2500	1	0.2500	1.21	0.3083	
BC	0.0000	1	0.0000	0.0000	1.0000	
A^2	0.0105	1	0.0105	0.0508	0.8281	
B^2	2.06	1	2.06	9.96	0.0160	
C^2	2.69	1	2.69	13.01	0.0087	
Residual	1.45	7	0.2071			
Lack of Fit	0.2500	3	0.0833	0.2778	0.8395	not significant
Pure Error	1.20	4	0.3000			
Cor Total	76.24	16				

3.3.2. Diagnostic plot

Figures 10a and 10b illustrate the normal probability plot of the residuals, and the predicted versus actual. It was observed that the values are close to the straight line, which demonstrates that the model is accurate. For the predicted versus experimental, the points are also distributed closely to the diagonal line with an R^2 value of 0.894. Thus, the model gives a good explanation of how the analysis of the variance of the response works. This is in agreement with the works of [53].

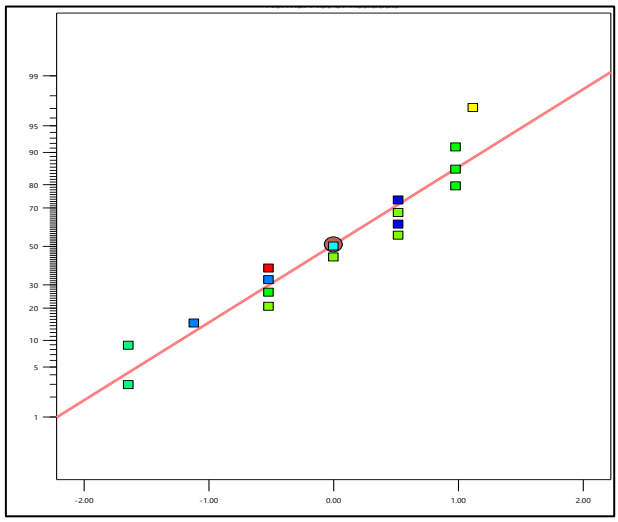

Figure 10a Normal % probability plot of MG-Si model

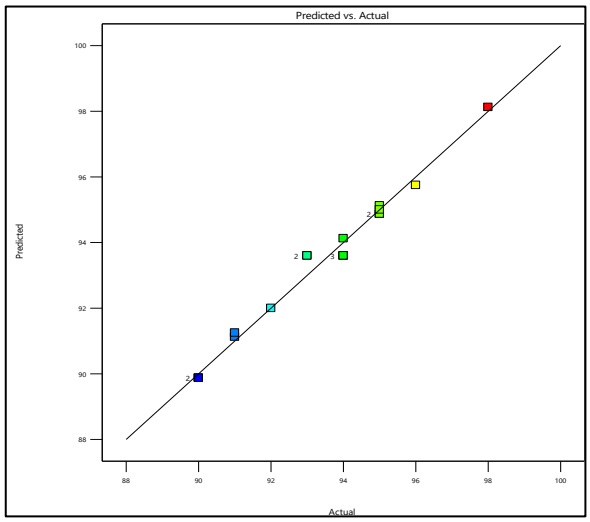

Figure 10b A plot of predicted vs experimental value

3.3.3. Model Equation

A model Equation serves as a mathematical representation that explains the connection between the factors and the resultant yield. In this instance, Equation 11 demonstrates that a quadratic model adequately predicts the metallurgical-grade silicon (MG-Si) yield.

MG-Si Yield = 93.6 2.25 A + 1.875B+0.375C -0.2500AB - 0.25AC + 0BC - 0.0500 A^2 + 0.7 B^2 - 0.8C^2..... Eq. 11

Where MG-Si Yield is metallurgical grade silicon yield, A is the calcination temperature, B is the ratio of HF:H_2SO_4, and C is the RHA:Mg.

3.3.4. Response Surface Plot for (MG-Si) Yield

This section discussed the interactive effect of the three factors on the MG-Si yield of the silicon. The model Equation developed was employed for generating the 3D response surfaces to better understand the interplay between the process factors and identify the optimum condition of each component for the production of silicon MG-Si of metallurgical grade. Figure 11a shows the significant interaction term for Ratio of HF:H_2SO_4 and calcination temperature indicating that these two factors affect the percentage yield of MG-Si. The results revealed that there is an increase in the yield of MG-Si with an increase in FH:H_2S0_4 ratio. Similarly, increased calcination temperature increases the MG-Si yield. Thus this is in agreement with the findings of Larbi, [11] who previously studied the effect of calcination temperature and reaction time on silicon yield from rice husk and attributed the outcome to the process of complete combustion. Conversely, this pattern of graph was also observed in the work of Ali, [54]. The effect of the interaction of the HF:H_2SO_4 ratio and calcination temperature on MG-Si yield can be seen in the 3D response surface plot shown in Figure 11b. it is observed that an increase in the RHA:Mg ratio results in a slight increase in the MG Si yield but at point 1.6, the yield is observed to drop very slightly, this may be because the ratio of RMA:Mg has reached its optimum potential, at this point, it is believed the reaction must have reached an equilibrium point, and a further increase in the RHA:Mg ratio will reduce the yield of the MG Si. Also, it was noticed that the highest MG-Si yields from the rice husk ash were obtained at an RHA:Mg ratio of between 1.4 to 1.8 and a calcination temperature of 800^{o}c. Thus, from the results obtained, it can be inferred that these findings correspond with the report of Kim and Choi, [55] and Olawale, [2] who report a similar trend in their work.

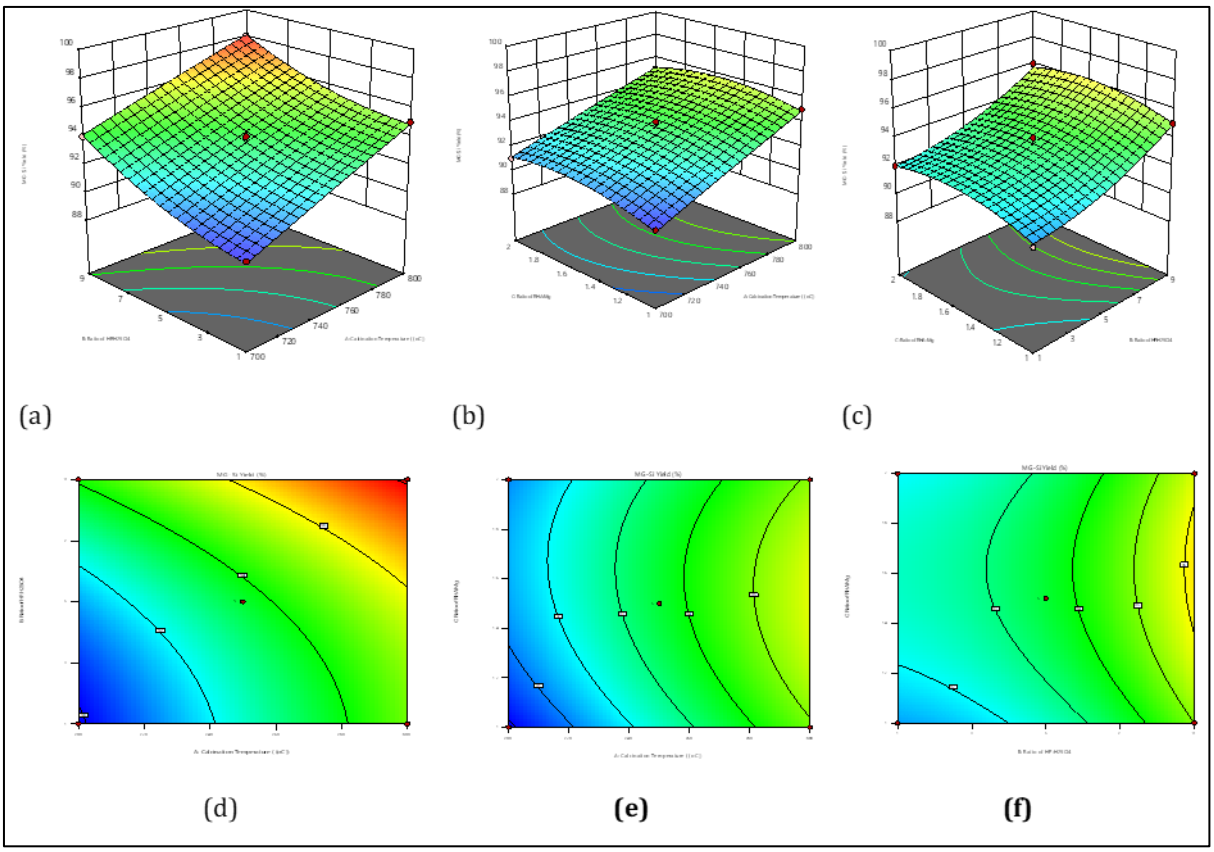

Figure 11 3D plot showing the effect of the independent variables on the yield of MG-Si: (a) shows 3D plot of Ratio of HF: H_2SO_4 and calcination temperature on MG-Si yield (b) 3D plot of RHA: Mg ratio and calcination temperature on MG-Si yield. (c) 3D plot of RHA: Mg ratio and Ratio of HF:H_2SO_4 on MG-Si yield

The interaction of the RHA: Mg ratio and HF:H_2SO_4 ratio on the MG-Si yield is shown in Figure 11c, based on the results of the ANOVA model. HF:H_2SO_4 ratio is observed to have a significant effect on the MG-Si yield. A careful observation of Figure 11c showed that MG-Si yields increased gently at the initial ratio of between 1 to 3, and later increased drastically from ratio 5 to 9 and attained a maximum MG-Si yield at 1:9 HF:H_2SO_4. Also, it is observed that an increase in the RHA:Mg ratio results in a slight increase in the MG-Si yield but at point 1.6, the yield is observed to drop very slightly, this may be because the ratio of HF:H_2SO_4. Thus, this is slightly different from the work reported by Ali, [54].

3.3.5. Numerical Optimization of (MG-Si) Yield

The operating parameters of the metallurgical-grade silicon production process were optimized numerically with the Design Expert version 13 to obtain optimal parameters and responses. All the operating parameters are in range. The optimization aimed at increasing metallurgical-grade silicon (MG-Si) yield and 10 solutions of optimization are presented in Table 7.

Table 7 Optimum value for MG-Si Yield

Number	Calcination Temperature	Ratio of HF:H_2SO_4	Ratio of RHA:Mg	MG-Si Yield	Desirability	
1	704.301	6.029	1.265	91.630	1.000	Selected
2	700.000	1.000	1.500	89.875	1.000	
3	700.000	9.000	1.500	94.125	1.000	
4	800.000	1.000	1.500	94.875	1.000	
5	750.000	9.000	1.000	95.000	1.000	

As indicated in Table 7, the Response Surface Method identified 10 solutions and chose optimal values to minimize the economic costs associated with calcination temperature, HF:H_2SO_4 ratio, and RHA: Mg ratio needed for the extraction of MG-Si while maximizing MG-Si yield. The selected optimum conditions resulted in metallurgical-grade silicon (MG-Si) yield of 91.630wt%, achieved at a calcination temperature of 704.301 °C, HF:H_2SO_4 ratio of 1:6.029 and ratio of RHA: Mg (1:1.265). Thus, the optimization was able to maximize MG-Si yield with the highest desirability of 1.000.

3.4. Artificial neural network model for Metallurgical-Grade Silicon (MG-Si) Yield

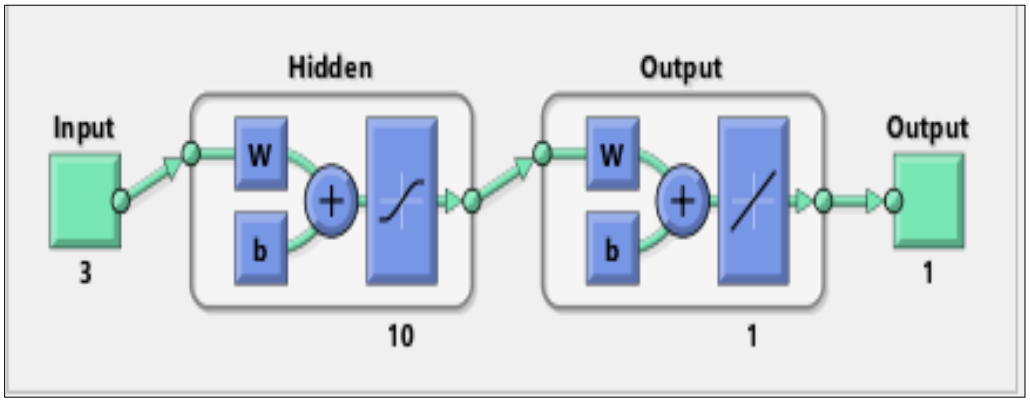

Figure 12 ANN architecture of the metallurgical-grade silicon (MG-Si) process

The network training process was iterated several times to ensure that the model predictions were consistent. Thus, the developed ANN model is a three-layer (i.e., input, hidden and output layers) feed-forward network with 6 neurons in the hidden layer as shown in Figure 12. As earlier mentioned, the training algorithm—Levenberg Marquardt was the best design for training the neural network as the mean square error (MSE) obtained was 0.0019046 at 1 epoch (iterations).

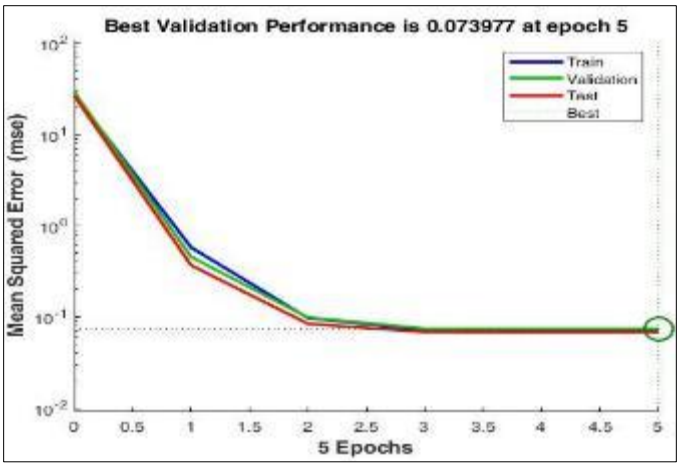

Figure 13 ANN performance validation plot

The reliability of the training process was evaluated using the validation performance plot in Figure 13, which showed the variation of the mean square error with the number of epochs for the optimal system. The training network showed the lowest validation mean square error (MSE) of about 0.0012 at the 5th epoch iteration. The MSE was very small showing that the trained network did not experience any over-fitting problem. If the test curve had increased significantly before the validation curve increased, then it could be possible that some over fitting might have occurred.

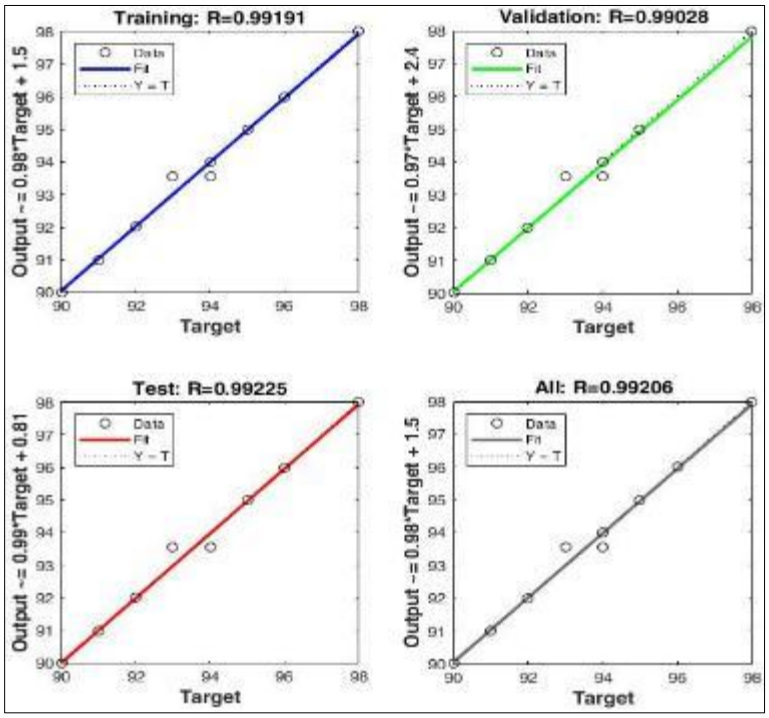

Figure 14 Artificial Neural Network (ANN) correlation plots for (a) training, (b) Validation, (c) testing and (d) overall network processes

The ANN regression plots that display the network target data (experimental) and the predicted output for training, validation, testing, and overall data are presented in Figure 14. The correlations obtained were 0.99191, 0.99028, 0.99225, and 0.99206 for training, testing, validation, and overall data respectively while the training mean square error was 0.0711. The correlation coefficients were close to one (1) in all the data sets indicating that the fit was appropriate for all the data set. Furthermore, the fit line fell on the 45-degree line, especially for the validation and the overall data sets where the targets were almost equal to the network outputs. Therefore, the ANN output network response was adequate in describing the yield of metallurgical-grade silicon (MG-Si) from rice husks ash (RHA).

3.4.1. Artificial Neural Network Model, Weights and Biases

From the results obtained, Equation 12 represents the trained ANN model for predicting (MG-Si) yield as output data from input parameters datasets, Calcination temperature (T_c), ratio of HF: H_2SO_4,(R_{HF}), and ratio of RHA: Mg(R_{RHA}). Equation 12 displays the empirical Equation for MG-Si yield prediction in normalized form, which is based on the Levenberg–Marquardt method.

$$(\mathrm{MG-Si})\text{yield} = \sum_{j=1}^{3}\left[purelin\left\{\sum_{i}^{10}\sum_{j=1}^{3} tangsig\left[(T_c IW_1 + R_{HF} IW_2 + R_{RHA} IW_3) + b_i\right]\right\} \times LW + b_{k1}\right] \ldots\ldots \quad \text{Eq. 12}$$

Tansig computed the layer's output from the network input, while the transfer function "purelin" correlated the linear connection between the input and output variables [56]. Thus, the tansig activation function is mathematically as:

$$(\tan sig = 2/(\{1 + \exp(-2\text{network})\} - 1) \quad \ldots\ldots\ldots\ldots \text{Eq. 13}$$

The variables IW_1, IW_2, and IW_3 are input weights attached to the Calcination temperature, ratio of HF: H_2SO_4, and ratio of RHA: Mg, respectively, from the input layer to the hidden layer. Also, LW is a hidden layer weight attached to the output layer. The variables bi and bk represent biases associated with the hidden layer neurones and output layer neurones, respectively. Table 8 shows the values for the developed ANN model's weights and biases. Using the model, weights, and biases of the developed ANN model as inputs, the model predicts the (MG-Si) yield by providing the following input variables: Tc, RHF, and RRHA values which then multiply with input layer weights IW1, for Calcination temperature, IW_2 for ratio of HF: H_2SO_4 and IW_3 for Ratio of RHA:Mg. For instance, the first (upper) neuron in the hidden layer can be evaluated as shown in Equation 14, using the values presented in Table 8.

$$(\mathrm{MG-Si})\text{yield} = \sum_{j=1}^{3}\left[purelin\left\{\sum_{i}^{10}\sum_{j=1}^{3} tangsig\left[(T_c(-2.19082) + R_{HF}(1.288478) + R_{RHA}(-1.78848)) + 2.89079\right]\right\} \times 0.045374 + 0.593866\right] \quad \ldots\ldots\ldots\ldots\text{Eq. 14}$$

Where IW_1= -2.19082, IW_2 = 1.288478, IW_3= -1.78848, LW=0.045374and b_1= 2.89079, and bki= 0.048663, the corresponding input logs (T_C, RHF and RRHA) values. Also, the network evaluates the other neurons in the hidden layer (i.e., i = 2, ...10), based on the mentioned procedure using their corresponding i, j values presented in Table 8.

Table 8 Weights and biases of the developed ANN model

	Input weight			**Hidden layer weight**	**Input layer biases**	**0utput layer biases**
i	IW1	IW2	IW3	LW	b_1	b_{ki}
1	-2.19082	1.288478	-1.78848	0.045374	2.89079	0.048663
2	-0.54342	-2.70317	-1.5279	-0.11658	2.051218	
3	0.011998	-0.28292	2.970604	-0.20627	-1.71104	
4	-1.74499	1.993087	-1.46848	-0.27948	0.45569	
5	-1.41878	0.255629	2.763776	0.149288	0.004739	
6	1.710316	0.111428	2.421603	0.429493	0.527694	
7	-2.10497	-0.84214	1.98762	0.041308	-1.6586	
8	2.044602	-0.02538	-2.17912	-0.38127	1.665156	
9	1.554268	1.264937	-2.36923	0.707365	2.282329	
10	1.039663	2.233199	-2.01944	0.676122	-2.97258	

Comparative analysis of the models

The accuracy of RSM, and ANN models in capturing the nonlinear nature of the metallurgical-grade silicon production process was evaluated using graphical and statistical methods. Generally, the two models were effective and near accurate in predicting the yield of metallurgical-grade silicon (MG-Si) using the silica extracted from rice husks ash. The result showed a close approximation between the experimental value and the RSM, and ANN model predictions which resulted in low residual values as shown in Figure 7. However, the ANN model seems to be more appropriate in

predicting the percentage of the yield of metallurgical-grade silicon (MG-Si), based on many insignificant values in their residuals.

Table 9 Comparison of RSM and ANN Models

S/N	Process Conditions			Percentage yield of MG-Si (%)		
	Calcination Temperature	Ratio of $HF:H_2SO_4$	Ratio of RHA:Mg	Experimental	RSM Model Predictions	ANN Model Predictions
1	750	5	1.5	94	93.60	94.50
2	750	5	1.5	93	93.60	94.50
3	750	5	1.5	94	93.60	94.50
4	800	5	1	95	94.88	85.77
5	800	9	1.5	98	98.12	89.99
6	800	5	2	95	95.13	89.46
7	750	1	1	91	91.25	96.99
8	750	5	1.5	93	93.60	94.50
9	700	9	1.5	94	94.13	94.00
10	750	1	2	92	92.00	96.00
11	750	5	1.5	94	93.60	94.50
12	800	1	1.5	95	94.88	93.01
13	750	9	2	96	95.75	92.00
14	700	1	1.5	90	89.87	99.15
15	700	5	2	91	91.13	95.95
16	700	5	1	90	89.88	91.59
17	750	9	1	95	95.00	93.02

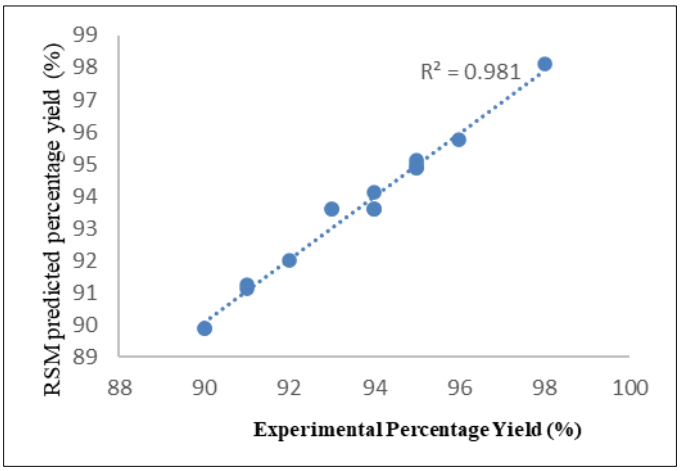

Figure 15a Comparative plots of experimental data and RSM percentage yield of MG-Si

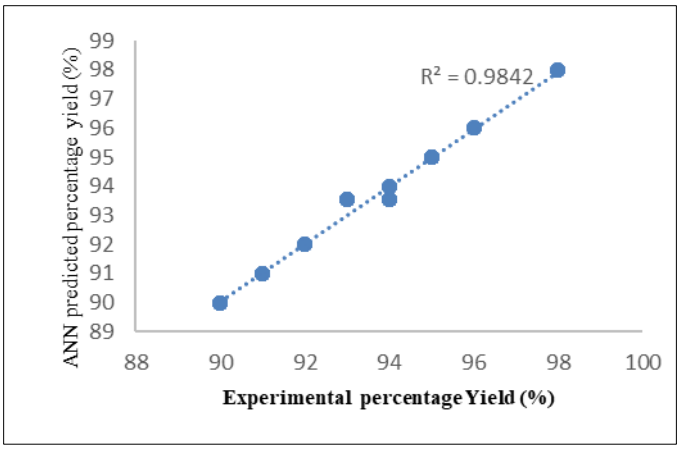

Figure 15b Comparative plots of experimental data with (a) RSM, and (b) ANN predicted yield of percentage MG-Si.

Fig. 15a-b showed the comparing plots, which showed a visual relationship between the experimental value and the model predictions made by ANN and RSM. The plots revealed a good fit between all of the suggested models and the experimental findings. The majority of the modes' factorial and axial points showed no substantial variance. The three models were then compared using statistical error functions.

3.5. Statistical Error Analysis

To further explore the model's precision abilities, five statistical error functions were applied to the model predictions with the values presented in Table 10. R^2, MAE, MSE, RMSE, and AAE which are the coefficient of determination, the mean absolute error, the mean square error, the root mean square error, and the average absolute error, respectively were evaluated for each model. Low values of these error functions depicted good predictive ability of the model. The result indicated negligible error values for all the models. In addition to these, R^2 was also evaluated for the models. Adepoju. [57] Asserted that the value of R^2 must not be less than 0.8 for reliable correlation involving predicted and experimental values. Thus, the result obtained was satisfactorily high for all the models, validating their importance. The higher the values of the R^2 the better the model predictions.

Furthermore, the RMSE and MSE square root were evaluated and the values obtained for MSE and RMSE were low, confirming that the models used are within range. AAE and MAE calculate a model's precision and accuracy as displayed in Tables 10. The model of ANN was able to predict metallurgical-grade silicon production more closely based on statistical index results. In general, the statistical results showed that the RSM was the least effective model in the prediction accuracy of the yield of the metallurgical-grade silicon (MG-Si) process. In contrast, the ANN model was marginally superior to the RSM model. The findings in the present study were in agreement with the works of Iyen *et al.* [1] and Larbi, [5], who all reported similar trends.

Table 10 ANN and RSM prediction model error analysis for MG-Si Yield

Error analysis indicators	ANN	RSM
R^2	0.9841	0.9808
MAE	0.0011	0.0012
MSE	0.0710	0.0012
RMSE	0.2665	0.0343
AAE	<0.0001	<0.0001

4. Conclusion

The outcomes of this research hold profound implications for sustainable silicon production, offering a pathway toward leveraging agricultural waste as a valuable resource while concurrently addressing environmental concerns associated with traditional extraction methods. Moreover, the insights gained from this study can inform policy initiatives and industrial practices aimed at fostering a circular economy by promoting the efficient utilization of agricultural by-

products. Also, the findings of this research hold significant implications for both industry and sustainability. Moreover, the development of optimized extraction processes aligns with the broader goal of reducing the environmental footprint of industrial activities and fostering sustainable practices.

Compliance with ethical standards

Acknowledgments

The authors will like to appreciate the managements of TETFUND for providing the fund and University of Uyo for the enabling environment to carry out this research work. This project was possible because of the provision of fund by Tertiary Education Trust Fund (TETFUND) Nigeria under the Institutional Based Research Grant number TETFUND/DR&D/CE/UNI/UYO/2020/RP/VOL.1.

Disclosure of conflict of interest

No conflict of interest to be disclosed.

References

[1] Iyen, C., Ayomanor, B.O., Mbah, V. (2020). Extraction and Processing of Crystalline Metallurgical-Grade Silicon Prepared from Rice Husk Byproduct. In: Chen, X., et al. Energy Technology 2020: Recycling, Carbon Dioxide Management, and Other Technologies. The Minerals, Metals and Materials Series. Springer, Cham. https://doi.org/10.1007/978-3-030-36830-2_21.

[2] Olawale, O., Akinyemi, B., Ogundipe S., Abayomi, S., and Adekunle, A. (2021). Response surface methodology for silicon production from bamboo leaves, International Conference on Energy and Sustainable Environment, IOP Conf. Series: Earth and Environmental Science 665, 012075.

[3] Swanson, R. M. (2006). A vision for crystalline silicon photovoltaics. Prog Photovoltaics Res Appl 14:443–453.

[4] Oboh, I. O., Ihom, A. P and Markson. I. E. (2023). Use of Rice Husk and Rice Husk Ash for Metallurgical Grade Silicon: The Production, Purification and Upgrade, International Journal of Engineering and Modern Technology (IJEMT). 9(1):2695-2149.

[5] Larbi KK, Barati M, McLean A (2011). Reduction behaviour of rice husk ash for preparation of high-purity silicon. Can Metal Q 50:341–349.

[6] Ding, M. (1992). Rice husk silicon and its applications. *Inorg. Chem. Ind*. 24 (6), 36.

[7] Pizzini, S. (2012). Advanced silicon materials for photovoltaic applications (pp. 311-353). John Wiley and Sons.

[8] Sun, L and Gong, K. (2001). "Silicon-based materials from rice husks and their applications," *Industrial and engineering chemistry research*, vol. 40, no. 25, pp. 5861-5877.

[9] Bakar, P.A. Rosiyah, Y. Seng, N.G. (2016). High Purity Amorphous Silica from Rice Husk. Proceedia Chemistry. vol. 19, pp189-195.

[10] Asly, K. (2008). Properties and behavior of quartz for the silicon process PhD dissertation, Norwegian University of Science and Technology, Trondheim.

[11] Larbi KK, Roy R, Barati M, Lakshmanan VI, Sridhar R, Mclean A. (2012). Use of rice husk for emission neutral energy generation and synthesis of solar-grade silicon feedstock. Biomass Conv Biorefinery 2:149–157.

[12] Pang, D; Weng, W; Zhou, J; Gu, D. and Xiao, W. (2021). Controllable conversion of rice husks to Si/C and SiC/C composites in molten salts. Journal of Energy Chemistry 55: 102–107.

[13] Usman, A. M. Raji, N. H. Waziri, and M. A. Hassan, "Aluminium alloy-rice husk ash composites production and analysis," *Leonardo Electronic Journal of Practices and Technologies,* vol. 25, pp. 84-98, 2014.

[14] Swatsitang, E., Srijaranai, S., and Arayarat, P. (2004). Preparation of Silicon from Rice Hulls, *Technical Digest of the International (PVSEC)*, 14, p. 301.

[15] Swatsitang, E. and Krochai, M. (2009). Preparation and Characterization of Silicon from Rice Hulls, *J. Met. Mater*. Miner, vol. 19, no. 2, p. 91.

[16] Hu, L., Wang, Z., Gong, X., Guo, Z., and Zhang, H. (2013). Impurities removal from metallurgical-grade silicon by combined Sn-Si and Al-Si refining processes. Metallurgical and Materials Transactions B, 44(4), 828-836.

[17] Onojah, A., Amah, A.N. and Ayomanor, B.O., (2012). Comparative studies of silicon from rice husk ash and natural quartz. Am. J. Sci. Ind. Res., 3(3): 146-149.

[18] Bangwar, D. K. Saand, A., Keerio, M. A., Soomro, M. A and Bhatti, N. (2017). "Development of an amorphous silica from rice husk waste. Engineering," *Technology and Applied Science Research*, vol. 7, no. 6, pp. 2184-2188.

[19] Barati, M. Larbi, K. K; Roy, R; Lakshmanan, V I; Sridhar, R (2011). Production of high purity silicon from amorphous silica, WO Patent 2,011,022,817.

[20] Nersisyan, H.H., and Won, H.I. (2011). Solar-grade silicon Powder Prepared by Combining Combustion Synthesis with Hydrometallurgy, Solar Energy Materials and Solar Cells, 95: 745–750.

[21] Yuge N., Baba H., Sakaguchi Y., Nishikawa K., Terashima H. and Aratani F. (1994). Purification of metallurgical silicon up to solar grade. Solar Energy Materials and Solar Cells, 34;243-250.

[22] Olusesi, O. S. and Udoye. N. E. (2021). "Development and characterization of AA6061 aluminium alloy/clay and rice husk ash composite," *Manufacturing Letters*, vol. 29, pp. 34-4.

[23] Chakravarthy, M. P. and D. Santha Rao, "Evaluation of mechanical properties of aluminium alloy (AA 6082) reinforced with rice husk ash (RHA) and boron carbide (B 4C) hybrid metal matrix composites using stir casting method," Materials Today: Proceedings, vol. 66, pp. 580-586, 2022.

[24] Costa, J.A.S.and Paranhos. C. M. (2018). *Systematic evaluation of amorphous silica production from rice husk ashes. Journal of Cleaner Production.*

[25] Islam, T; Hossen, F; Asraf a, A; Zahan, K. E. and Zakaria, C. M. (2024). Production and Characterization of Silica from Rice Husk: An Updated Review. *Asian Journal of Chemical Sciences*, 14(2): 83-96

[26] Abdullah, M. N., Mustapha, N. Sallih, A. Ahmad, F. Mustapha, and A. Dahliyanti, "Study and use of rice husk ash as a source of aluminosilicate in refractory coating," *Materials (Basel)*, vol. 14, no. 13, p. 3440, 2021.

[27] Dhaneswara, D., Jaka Fajar, F., Wensten, F., Situmorang, H. (2020). Synthesis of Amorphous Silica from Rice Husk Ash: Comparing HCl and CH_3COOH Acidification Methods and Various Alkaline Concentrations, *International Journal of Technology*, 11(1) 200-208.

[28] Kalapathy, U., Proctor, A. and Shultz, J. (2000). "A simple method for production of pure silica from rice hull ash," Bioresource Technology, vol. 73, pp. 257-264.

[29] Riveros H and Garza C. (1986). Rice husks as a source of high purity silica. Journal of Crystal Growth.;75(1):126-131.

[30] Giginyu, I. M. and Shuaibu Z. Y. (2023) Many rice mills shut down production over paddy scarcity. Daily trust 20/08/ 2023 available at: https://dailytrust.com/many-rice-mills-shut-down-production-over-paddy-scarcity/

[31] Enoch, D.O. Akintunde, A.A. Adewale, A.O. (2018). A Review on Recent Studies on Development of Rice Husk Silica and Its Application in Thin Film Growth. International Journal of Nanoscience and Nanoengineering vol 4 issue 4 pp 74-79.

[32] Benedict, O., A and Karen, V. (2015).Potential Synthesis of Solar-Grade Silicon from Rice Husk Ash, Solid State Phenomena, Vol. 242, pp 41-47.

[33] Singh R, Dhindaw BK. (1978). Production of high-purity silicon for use in solar cells. In: De Winter F, Cox M (eds) Sun, Mankind's Future Source of Energy: Proceedings of the International Solar Energy Congress. Pergamon Press, New York, pp 776–781.

[34] Bose, D. N; Govindacharyulu, P A. (1984) Progress in solar-grade silicon from rice husk ash. Pergamon press, perth, pp. 2735 - 2781.

[35] Banerjee, H. D., Sen, S. N. and Acharya, H. N. (1982). Investigations on the production of Silicon from rice husks by the Magnesium method. Journal of Material Science and Engineering. 52:173-179.

[36] Ikram N, Akhter M. (1988). X-ray diffraction analysis of silicon prepared from rice husk ash. *J Mater Sci* 23:2379–2381.

[37] Pires J.C.S., Otubo J., Braga A.F.B. and Mei P.R. (2005). The purification of metallurgical grade silicon by electron beam melting. *J. Mater. Process. Technol*., 169; 6-20.

[38] Liou, T. H and Wang, P.-Y. "Utilization of rice husk wastes in synthesis of graphene oxide-based carbonaceous nanocomposites," *Waste management*, vol. 108, pp. 51-61, 2020.

[39] Saleh, M., Demir, D., Ozay, Y., Yalvac, M., Bolgen, N. and Dizge, N. (2021b) Fabrication of basalt embedded composite fber membrane using electrospinning method and response surface methodology. Journal of Applied Polymer Science 138:50599

[40] Rafiee, E., Shahebrahimi, S., Feyzi, M., and Shaterzadeh, M. (2012). Optimization of synthesis and characterization of nano silica produced from rice husk (a common waste material). *International Nano Letters*, 2:29.

[41] Rahmanian, B., Pakizeh, M., Mansoori S. A., Abedini R. (2011). Application of experimental design approach and artificial neural network (ANN) for the determination of potential micellar-enhanced ultrafiltration process. *J. Hazard. Mater*. 2011; 187:67–74.

[42] Elfghi F.M. (2016). A hybrid statistical approach for modeling and optimization of RON: A comparative study and combined application of response surface methodology (RSM) and artificial neural network (ANN) based on design of experiment (DOE) Chem. Eng. Res. Des. 2016; 113:264–272.

[43] Umeda, J and Kondon k. (2008). Process optimization to prepare high-purity amorphous silica from rice husks via citric acid leaching treatment. *Transactions of JWRI.* 37:13-17.

[44] Asadi, S and Moeinpour, F. (2019). "Inactivation of Escherichia coli in water by silver-coated NiO. 5ZnO. 5Fe 2 O 4 magnetic nanocomposite: a Box-Behnken design optimization," *Applied Water Science*, vol. 9, no. 1, pp. 1-9.

[45] Manojkumar N, Muthukumaran C, Sharmila G. (2020). A comprehensive review on the application of response surface methodology for optimization of biodiesel production using different oil sources. *J King Saud Univ-Eng Sci.*, 34(3):198–208.

[46] Senthilkumar C, Krishnaraj C, Sivakumar P, Sircar A. (2019). Statistical optimization and kinetic study on biodiesel production from a potential non-edible bio-oil of wild radish. *Chem Eng Commun.,* 206:909–18.

[47] Yusuff AS, Popoola LT, Adeniyi OD, Olutoye MA. (2022). Coal fly ash supported ZnO catalyzed transesterification of Jatropha curcas oil: optimization by response surface methodology. Energy Conv Manag X.

[48] Desai, K. M., Survase, S. A., Saudagar, P. S., Lele, S. S., Singhal, R. S. Comparison of artificial neural network (ANN) and response surface methodology (RSM) in fermentation media optimization: Case study of fermentative production of scleroglucan. Biochem. Eng. J. 2008; 41:266–273.

[49] Azevedo, B.F., Rocha, A.M.A.C. & Pereira, A.I. Hybrid approaches to optimization and machine learning methods: a systematic literature review. *Mach Learn* 113, 4055–4097 (2024).

[50] Abdullahi, K; Ojonugwa, S. S; Yusuff, A. S; Umaru, M; Mohammed; I.A; Olutoye, M. A. and Aberuagba, F. (2023). Optimization of biodiesel production from Allamanda Seed Oil using design of experiment. Fuel Communications 14: 1–9

[51] Zaghloul, M.S. Hamza, R.A. Terna, I.O. Tay J.H. (2020). Comparison of adaptive neuro-fuzzy inference systems (ANFIS) and support vector regression (SVR) for data-driven modelling of aerobic granular sludge reactors J. Environ. Chem. Eng., 10.1016/j.jece.2020.103742

[52] Onu, C. Elijah., Nwabanne, J. T., Ohale, P. E., and Asadu, C. O. (2020) "Comparative analysis of RSM, ANN and ANFIS and the mechanistic modeling in eriochrome black-T dye adsorption using modified clay", *South African Journal of Chemical Engineering,*36: 24-42

[53] Majdi, H; Esfahani, J. A. and Mohebbi, M. (2019). Optimization of convective drying by response surface methodology. Computers and Electronics in Agriculture, 156(), 574–584.

[54] Ali, H. H. M., El-Sadek, M. H., Morsi, M. B., El-Barawy, K. A. and Abou-Shahba, R. M. (2018). Production of metallurgical-grade silicon from Egyptian quartz. Journal of the Southern African Institute of Mining and Metallurgy, 118(2), 143-148.

[55] Kim, J and Choi, J., Choi, O. (2017). Effects of adolescent smartphone addiction on cybersexual delinquency. Social Behavior and Personality, 45(5), 819–831. https:// doi.org/10.2224/sbp.5916.

[56] Okon, A. N, Idongesit, B. A. (2021) "Artificial neural network models for reservoir-aquifer dimensionless variables: influx and pressure prediction for water influx calculation", Journal of Petroleum Exploration and Production Technology.

[57] Adepoju, T. F., Esu, I. O., O. A. Olu-Arotiowa , E. Blessed (2019). Oil Extraction from Butter Fruit (Dacryodes Edulis) Seeds and its Optimization via Response Surface and Artificial Neural Network. Nigerian journal of technological development, 16(2); 56-62.